SEYBOLD Report
ISSN: 1533 - 9211
DOI: 10.5281/zenodo.7236067

SYNTHESIS OF CERIUM OXIDE NANOPARTICLES AND THEIR SURFACE MORPHOLOGY EFFECT ON BIOLOGICAL ACTIVITIES

M. Charumathy
Research Coordinator & Assistant Professor, PG & Research Department of Biochemistry, Marudhar Kesari Jain College for Women, Vaniyambadi, Tamil Nadu,
Email: mcharumathy4@gmail.com

Masma Shaik
Assistant professor, Department of S&H, St. Peters Engineering college, Hyderabad,
Email: shaheenshaik186@gmail.com

S. Violet Beaulah
Assistant Professor, Department of Microbiology, Rathinam College of Arts and science, Coimbatore, Tamil Nadu, Email: beaulahsam@gmail.com

Gaurav Singh
Assistant Professor, Department of S&H, St. Peter's Engineering College, Hyderabad,
Email: gauravnanotechnology@gmail.com

P. Priyadarshini,
Associate Professor, Department of Microbiology, Justice Basheer Ahmed Sayeed College for Women, Chennai, Tamil Nadu, Email: priyadarshini.p@jbascollege.edu.in

G.Veeramalai
Assistant Professor, Department of Mathematics, M.Kumarasamy College of Engineering (Autonomous), Thalavapalayam, Tamil Nadu, Email: veeramusiri@gmail.com

ABSTRACT:

Here, the trustworthy work has been completed for the hydrothermal and co-precipitation methods of synthesizing Cerium oxide (CeO_2) nanoparticles (NPs). We highlight the extremely effective hydrothermal approach for creating CeO_2 NPs for use in biological applications. Absorption Peaks at 283 nm and 274 nm in the spectra confirmed the production of CeO_2 NPs for the co-precipitation (CONPs) and hydrothermal (HYNPs) approaches, respectively. The results of functional group analysis clearly demonstrated the presence of both organic and inorganic species. Demonstrated that HYNPs and CONPs shared similar features. Cubic form and typical We estimate the crystallite size of produced NPs using Sherrer's and W-H techniques. Obtained HR-TEM is used to compare average particle size, which is around 10 nm and 5 nm for. Both HYNPs and CONPs are acceptable. Additionally, we investigated their antibacterial capacities.

Keywords: Cerium oxide; Co-precipitation; Gram bacteria; Hydrothermal; W-H method

SEYBOLD Report
ISSN: 1533 - 9211
DOI: 10.5281/zenodo.7236067

1. INTRODUCTION

Due to their distinctive and remarkable qualities, nano structural rare earth minerals have numerous applications. The rare earth inorganic rare earth's interfacial characteristics effects of nanoparticles on reaction rates through the size-dependent change in crystallinity of the surface nanoparticles. Due to their high surface tension, these materials Quantum size effect and volume to volume ratio at the nanoscale it increases the reactivity between surfaces [1] and good visual, mechanical, biological, and physical evidence and uses for catalysis [2, 3]. One of them is Cerium. a superior rare earth element. Nanoceria, in general is common because of their distinctive qualities, such as good Solid oxide fuel cells (SOFCs) use an oxide ion conductor [4] gas sensors [5] and. Additionally, they have wide band gap energy. which is true in order to due to its UV absorption, excellent thermal stability, toughness, and catalytic reactivity [6,7]. Although ceria can change their morphologies, has physicochemical characteristics that allow for an application UV light act as catalysts in an emission control system. sunscreen, solar cells, and blocking material make-up [8].

Recently, nanoceria were created utilising diverse techniques in an effort to enhance their physical-chemical properties. In addition to hydrothermal [9, 10], co-precipitation [11], reversed micelles reaction [12], template-assisted precipitation [12], sol-gel [13], spray drying system [14], plasma spray technique [15], microemulsion procedure [16], self-assembled system [17], solvothermal [18], and thermal decomposition [19], other significant methods include solvothermal and solvothermal. These techniques have all been used over the past few years to create CeO_2 nanostructures such as nanoparticles, nanorods, nanowires, nanotubes, nanocubes, and nanospheres. To create highly sensitive third generation biosensors, sol-gel produced CeO_2 NPs were investigated for their electrochemical and catalytic properties [20, 21]. CeO_2 NPs produced electrochemically are employed as sensors, either as the transducer or as a component of it [22]. Due to their high surface-to-volume ratio, the robust solution produced ultrathin CeO_2 NPs are exploited for high oxygen storage capacity [23]. High oxygen mobility and a large oxygen diffusion coefficient of CeO_2 NPs at the surface aid in changing the valence state of cerium, which subsequently permits oxygen to be released or retained [23]. Monodisperse hollow ceria spheres are created using a green method, which further improves photocatalytic activity [24]. CeO_2 nanoparticles were created, and numerous fields have benefited from their physical-chemical characteristics. Since a few years ago, CeO_2 NPs have been created, and their new features have been reported [22]. This has made CeO_2 NPs useful in the disciplines of bioanalysis and biomedicine. The burning of the solution combustion produced CeO_2 NPs are used in cancer treatment, biosensors, and retinopathy [25]. In addition, the creation of a new a specific kind of nanoceria displays interactions with molecules like lipids, anions, and proteins [26].

Due to CeO_2 NPs' promising antibacterial activity and mentioned regenerative antioxidant qualities, scientists have become increasingly interested in the medical field throughout the last decade [27]. Nano-sized fine cerium oxide crystallites are becoming a highly effective and practical material in many industries. However, there are several challenges in the manufacture of CeO_2 NPs, such as the high cost of production, high energy consumption, complex manufacturing method, and expensive raw materials. All of these motivated us to

SEYBOLD Report
ISSN: 1533 - 9211
DOI: 10.5281/zenodo.7236067

come up with fresh approaches for producing CeO_2 NPs in an efficient, one-step manner.

In this article, we concentrate on the hydrothermal and coprecipitation technique of CeO_2 NP synthesis. We provide a straightforward, environmentally friendly method. Spectral characteristic analysis of optical, functional group, morphological, compositional, and thermal behavior studies were performed on the samples after CeO_2 NPs were synthesized. The biological activities of both HYNPs and CONPs, specifically antimicrobial and antioxidant studies, are then analyzed based on these findings in order to determine which will be the most suited CeO_2 NPs for biomedical applications.

2. MATERIALS AND METHODS

It was possible to create cerium oxide (CeO_2) nanoparticles by co-precipitation and hydrothermal processes. The supplies used are listed below. Hexahydrate of cerium (III) nitrate

- ($Ce(NO_3)_3.6H_2O$)
- Pellets of sodium hydroxide (NaOH)
- Ethanol (CH_3CH_2OH)

The suppliers of the materials were HIMEDIA Laboratories Pvt. Ltd. in Mumbai, India. Without additional purification, A. R grade compounds were employed in their entirety. The suspension and solution were prepared using deionized water**.**

2.1 Synthesis of CeO_2 NPs

2.1a. Hydrothermal method

The process is as follows, in brief: 10 ml of deionized water were used to dissolve 4.34 gramme of Ce $(NO_3)_3$.6H2O (1 M). NaOH solution is made by dissolving 0.04 g of pellets of NaOH (0.1 M) in 10 ml of deionizer water. While stirring continuously, the produced NaOH solution was added to the cerium precursor in dropwise fashion. For a short period of time, both solution mixes were mixed at room temperature. The resultant light brown-colored solution was then transferred to a 25-cc stainless steel autoclave lined with Teflon. The autoclave was then sealed and heated for 3 hours at 180°C before being allowed to cool to room temperature. To eliminate organic molecules that were present on the product's surface, the precipitate was centrifuged once with ethanol and multiple times continuously with deionized water. The item was then heated to 60°C.Using a laboratory oven, evaporate the water content for 60 minutes. The resulting light brown powder from hydrothermal synthesis was used for additional characterisation procedures.

2.1b. Co-precipitation technique

To create CeO_2 nanoparticles, a cerium precursor was first synthesised by dissolving 2.17 g of $Ce(NO_3)_3$.6H2O (0.5 M) in 20 ml of deionized water, agitating the solution, and then adding 0.04 g of NaOH (0.1 M) to 5 ml of deionized water. Drop by drop, the NaOH solution was added to the swirling cerium precursor. For 30 minutes, the precursor and NaOH solution were constantly stirred. The resulting antique white solution was allowed to stand for a night to allow the particles to settle, after which the precipitate was centrifuged and repeatedly rinsed with deionized water and once with ethanol to remove organic contaminants. CeO_2 nanopowders were produced by heating the final product to 60 °C in a laboratory oven for 60

SEYBOLD Report
ISSN: 1533 - 9211
DOI: 10.5281/zenodo.7236067

minutes. This powder was then employed for additional characterisation procedures.

Figure 1 below displays a schematic diagram of the hydrothermal and co-precipitation approach used to create CeO_2 nanoparticles.

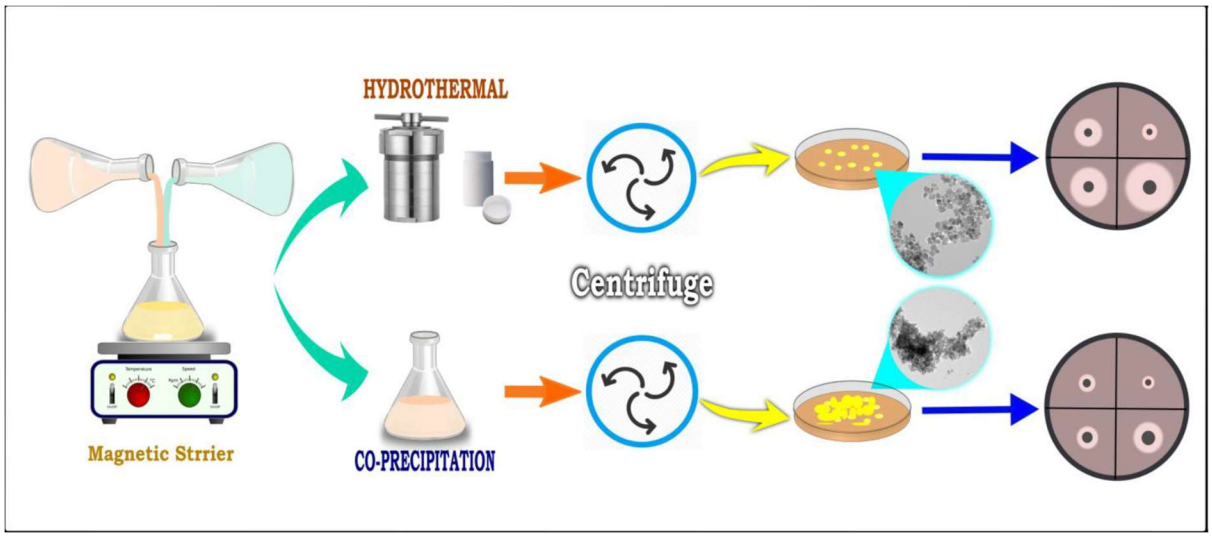

Figure - 1

2.2 Techniques for characterization

(2.2a). Energy band gap investigations

In order to analyse absorption maxima and energy band gaps, UV-Visible spectroscopy was used at K. U. Dharwad in Karnataka, India. UV-Vis spectra were taken in the wavelength range of 200 nm–600 nm using a UV-Vis spectrometer (model: V-670 Jasco).

(2.2b). Functional group analysis

Utilizing KBr powder, FT-IR absorption bands for synthesized CeO_2 NPs were captured. At USIC, K. U. Dharwad, Karnataka, India, the FT-IR was collected between 4000 cm-1 and 400 cm-1 using an FT-IR spectrophotometer (model: Nicolet 6700).

(2.2c). Grain size measured using a powder X-ray diffractometer (model: Shimadzu 7000), Cu-K radiation (=1.5406) and a scanning rate of 0.02 degrees per second in the range of 20° to 80°, CeO_2 NP crystal structure or phase evolution and crystallite size were examined. PCPDFWIN software was used to compare and evaluate the XRD peak data.

(2.2d). Surface morphological investigations

At an operating voltage of 200 kV, the particle size and shape of produced CeO2 NPs were investigated (Transmission Electron Microscopy) Jeol/JEM 2100) in Kerala, India, at STIC. Further, TEM pictures were examined using the PIXEL programme

(2.2e). Thermal and stability analysis

CeO_2 NPs' thermal stability and breakdown were studied. Employing thermogravimetric analysis to analyses (TGA) Differential scanning calorimetry (model: SDT Q600)(DSC) (model: Q20 V24.10 Build 122). (Model: Q20 V24.10 Build 122). TGA captured within the range from room temperature to 700°C. DSC data was captured between ambient and 500 °C at Indian state of Karnataka is home to USIC.

2.3 Biochemical processes

(2.3a). Antimicrobial activity

SEYBOLD Report
ISSN: 1533 - 9211
DOI: 10.5281/zenodo.7236067

The antimicrobial analysis employs the agar well diffusion method. Here, we tested the antimicrobial efficacy of five different microorganisms. For the antibacterial study, we used the Gram-positive bacteria Staphylococcus aureus and Bacillus subtilis, as well as the Gram-negative bacteria Escherichia coli and Pseudomonas aeruginosa. Candida albicans, a yeast, was utilised as an antifungal.100 l of the test organisms were initially swab inoculated onto the sterile Potato Dextrose agar petri plates for fungus and Nutrient Agar petri plates for bacteria before 4 wells were drilled. Four different concentrations of the produced CeO_2 NPs were deposited into each labelled well (125, 250, 375, and 500 g/ml in sterile distilled water). After the plates were incubated for 48 hours at 27°C for fungus and 24 hours at 37°C for bacteria Later, we must measure the Zones of Inhibition in mm (millimeter) using a scale in order to determine the antibacterial activity of the produced CeO_2 NPs.

(2.3b). Using the DPPH radical scavenging method, the antioxidant activity of CeO_2 nanoparticles is assessed.

The 1, 1-diphenyl-2-picrylhydrazyl (DPPH) technique was used to explore the antioxidant properties of the produced CeO_2 NPs, and it was evaluated based on its capacity to scavenge free radicals. The DPPH solution was created in accordance with our earlier paper [28]. Here, 2 ml of DPPH solution was added along with 1 ml of the produced CeO_2 NPs at various concentrations (100, 200, 300, 400, and 500 g/ml). Ascorbic acid was utilised as a reference (100, 200, 300, 400, and 500 g/ml). The control was a mixture of 2 ml of DPPH solution and 1 ml of distilled water. After being thoroughly blended, the reaction mixture was let to sit in the dark at room temperature for 30 minutes. At 517 nm, the absorbance was spectrophotometrically measured.

Equation 100 was used to calculate the antioxidant activity of the produced CeO_2 NPs based on the percentage of DPPH radical scavenging activity.

$$\%RSA = \frac{\text{control absorbance - sample absorban}}{\text{Control absorbance}} * 100$$

The studies were performed in triplicates, and one-way ANOVA was used to express the findings as mean standard deviation. The significance of the discrepancies between the Standard and created substances was ascertained using Turkey's multiple comparison tests. Using p=0.01, Pearson's correlation analysis was used to conduct the correlation analysis.

3. RESULT AND CONVERSATION

3.1 Studies of the energy band gap

UV-Vis spectrophotometer was used for the energy bandgap analyses, as well as for preliminary confirmation of the existence of CeO_2 material by looking at the absorption maxima (max) for both HYNPs and CONPs. The absorption maxima for the hydrothermal and co-precipitated methods were determined to be 283 nm and 274 nm, respectively, for CeO_2 NPs UV-Vis spectra in both cases, using ethanol as the solvent and ambient temperature (Figure 2(a)).

SEYBOLD Report
ISSN: 1533 - 9211
DOI: 10.5281/zenodo.7236067

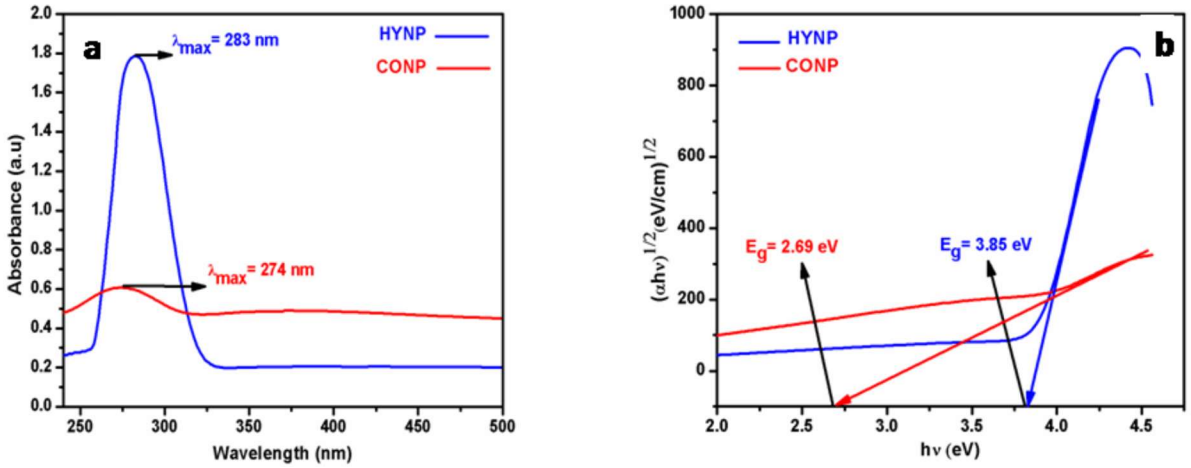

Figure 2(a). UV-vis spectra for HYNPs and CONPs, **(b)** Tauc's plot for HYNPs and CONPs

The Kubelka-Munk transformation method was used to measure the band gap energy of the CeO_2 NPs. Equation (1) uses the optical absorbance () as a function of the band gap energy () of artificial CeO_2 NPs. Where n is the nature of the transition, with n=1/2 for authorised direct transition and n=2 for allowed indirect transition [29, 30], and where A is a constant, with band gap energy. The direct bandgap energy for CeO_2 NPs was established by fitting the absorption data to the direct transition equation and plotting the ()2 Vs graph.

Figure 2 illustrates the estimated band gap of CeO_2 NPs produced by the hydrothermal and co-precipitation methods by extrapolating the linear component of the curve towards zero absorption, which results in direct transitions (b). This is often referred to as Tauc's scheme. The HYNPs and CONPs were found to have estimated direct band gaps of 3.85 eV and 2.69 eV, respectively.

3.2. Analysis of functional groups

The existence of functional groups was examined using Fourier transform infrared spectroscopy (FT-IR), which displays the distinctive vibration bands of organic and inorganic species. By using the KBr pellet method, the IR spectra of HYNPs and CONPs were obtained with a resolution of 2 cm-1 and ranged from 4000 cm-1 to 400 cm-1.

Figure 3 displays the FT-IR spectra of HYNPs and CONPs. Table 1 lists the IR bands that were observed. All vibration modes and both spectra are studied, and the results are in good accord with the literature [8, 31–33].

SEYBOLD Report
ISSN: 1533 - 9211
DOI: 10.5281/zenodo.7236067

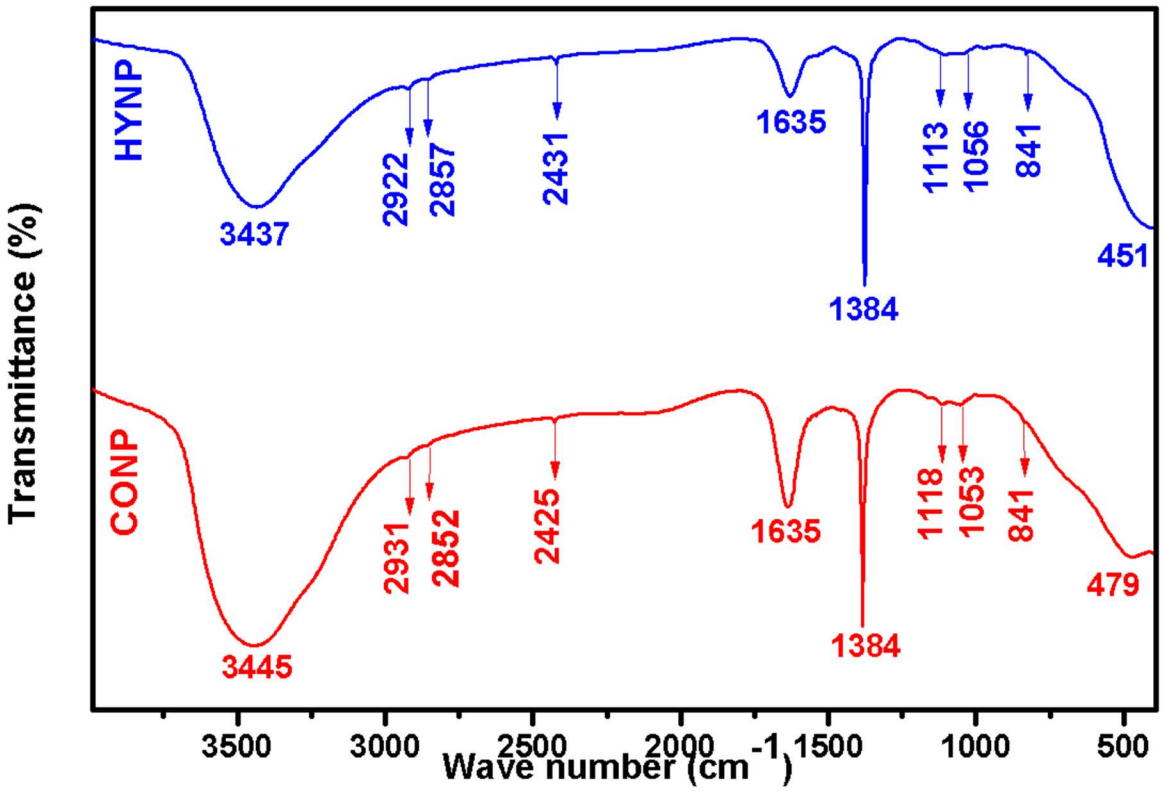

Figure 3. FT-IR spectra of HYNPs and CONPs

The fact that the identical chemicals are used in both ways of preparation means that the finished sample offers exceptional and desired outcomes. As a result, neither the peaks that actually occurred nor the main discrepancies between the spectra of HYNPs and CONPs are significantly altered.

3.3 Studies on grain size and structure

To ascertain the current crystallite phase of the produced CeO_2 NPs, X-ray diffraction (XRD) was employed. Figure 4(a) and (b) show the XRD patterns of CeO_2 NPs produced by the hydrothermal and co-precipitation methods, respectively. We noted a number of distinguishing peaks in the XRD pattern for CeO2 NPs produced hydrothermally. As for the coprecipitation method, they are as follows: 28.54(111), 33.05(200), 47.47(220), 56.33(311), 59.07(222), 69.40(400), 76.68(331), and 79.06(420). (331). These values relate to the Bragg's angle (2°) and the accompanying Bragg's reflection planes (hkl).

According to the Joint Committee on Powder Diffraction Standards (JCPDS file No. 81-0792), which indicated that synthesised CeO_2 NPs had a face-centered-cubic structure, these values are in agreement with that standard. The absence of further impurity peaks indicates that the high purity CeO_2 was produced. Additionally, the reflection peaks are distinct, therefore the average crystallite size of the sample was determined by broadening the X-ray line of reflections. To assess the average particle size of the CeO_2 NPs, XRD measurements can be used. Here, we used the broadening of peaks in the XRD pattern along with Scherrer analysis and the W-H method to determine the crystalline size.

3.3a. Scherrer's method for measuring crystallite size

SEYBOLD Report
ISSN: 1533 - 9211
DOI: 10.5281/zenodo.7236067

The X-ray diffraction peak was used to estimate the CeO_2 NPs' particle size. Using Scherrer's equation, we estimated the average particle sizes of CeO_2 NPs.

Where D denotes the average particle size, denotes the wavelength of Cu K radiation (0.15406 nm), k denotes the form factor (k=0.9), FWHM denotes the full width at half maximum, and denotes the peak's Bragg's angle. The line broadening of the most intense peak at plane (111), which is the crystallite's size, was calculated. For HYNPs and CONPs, the calculated average crystallite sizes are 9.53 nm and 5.4 nm, respectively.

3.3b. By using the William-Hall (W-H) method, crystallite size

Crystallite size and lattice strain are the other two independent characteristics that affect total peak broadening in addition to the X-ray peak broadening. W-H will pre sump that the strain is present and evenly distributed throughout the material. The relation s=4tanhkl gives the strain-induced line broadening, or s, that is seen. The sum of the contributions from crystallite size and material strain results in the overall peak broadening. Equation [34–37] provides the W–H equation for the uniform determination model.

Full-width half maximum (FWHM), Bragg's diffraction angle, shape factor, radiation wavelength, crystallite size, and lattice strain are all included in this equation. Fitting a plot using 4sin versus scos as seen in figures 4(c) and (d), respectively, for the hydrothermal and co-precipitation methods the intercept value of the plot is used to determine the crystalline size. The HYNPs and CONPs were calculated to be 9.66 nm and 7.02 nm, respectively, in size.

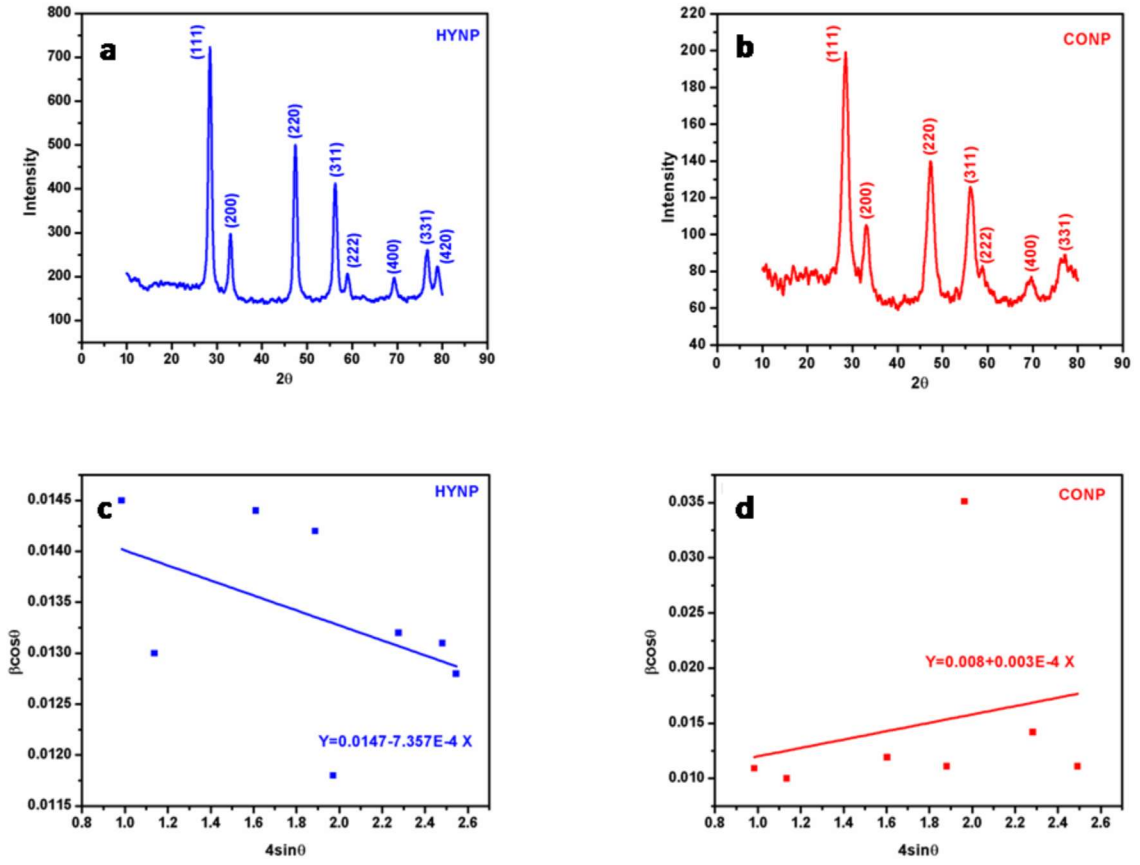

Figure 4(a). XRD pattern for HYNPs,**(b)** XRD pattern for CONPs, **(c)** W-H plot for HYNPs,

SEYBOLD Report
ISSN: 1533 - 9211
DOI: 10.5281/zenodo.7236067

(d) W-H plot for CONPs.

3.4 Studies on the surface morphology

Further TEM examination of the produced CeO_2 NPs' shape and nano nature was conducted. Figure 5(a), which depicts the TEM overall image of HYNPs, and Figure 5(b), which depicts the SAED pattern, both demonstrate the NPs' regular, uniform, and cubic morphology. The CeO_2 NPs are determined to be 10.5 nm in size on average. Figure 5(b) shows a brilliant spot and strong rings, which show that the sample is naturally well-crystallized. The CONPs TEM overview image is seen in Figure 5(c). We noticed that the size distribution in this figure is narrow and irregularly directed. It can be a sign that the CeO_2 NPs are properly crystallized.

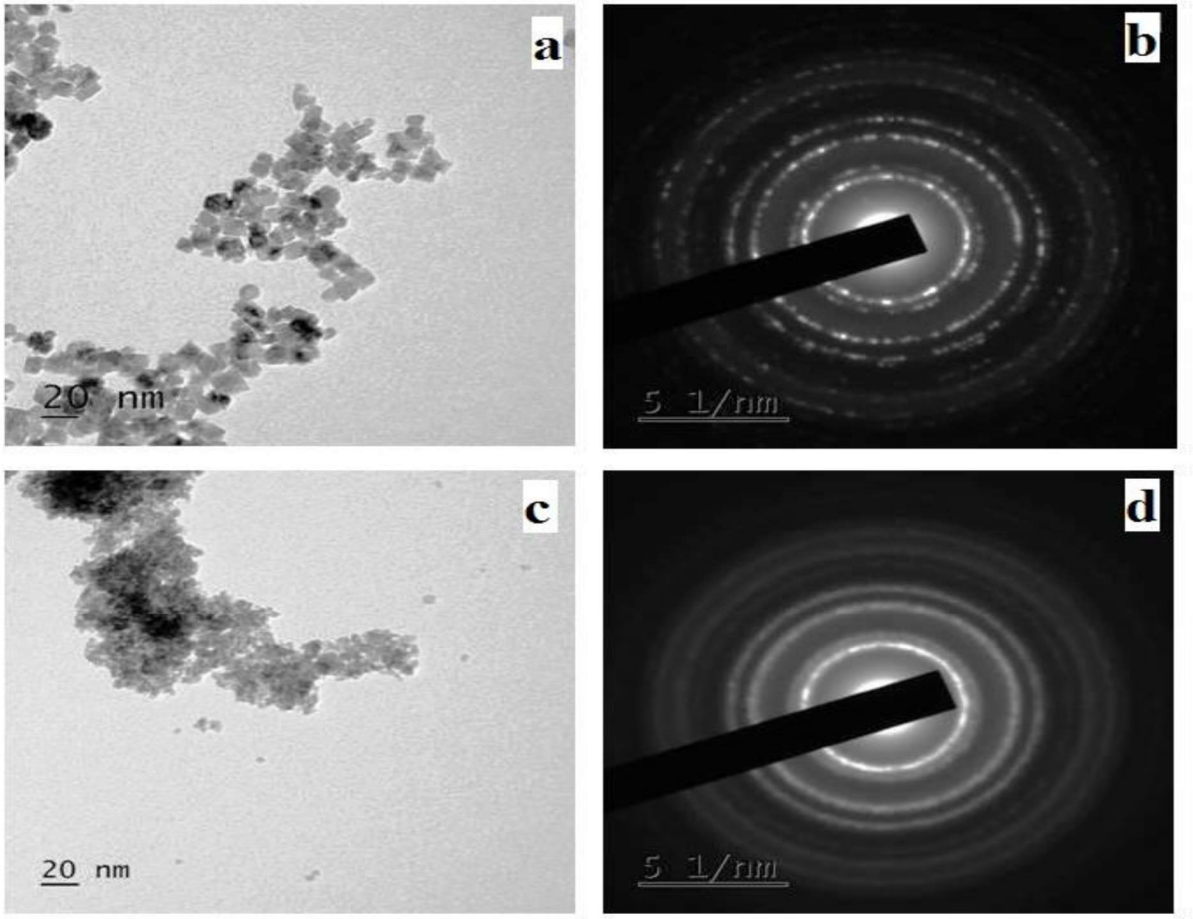

Figure - 5

But because the particles weren't dispersed in a solvent prior to sample preparation for TEM, the majority of the NPs were aggregated. CeO_2 NPs are discovered to have an average particle size of 5.78 nm. Figure 5(d) shows the SAED pattern of CONPs and rings in this image that may be CeO_2 structure reflections. The diffraction rings' broadening, which is less pronounced than in figure 5(d), indicates that the particles are tiny and or are of low crystalline type [8][37].

3.5. Stability and thermal analyses

We used differential scanning calorimetry (DSC) and thermogravimetric analysis

SEYBOLD Report
ISSN: 1533 - 9211
DOI: 10.5281/zenodo.7236067

(TGA) to examine the thermal properties of CeO_2 NPs (DSC). The sample was given a continuous heat rate of 10°C/min. It's crucial to carry out such a study with an inert gas to prevent any premature conclusions. About 5.5 mg of NPs were placed in a pan and heated to 700 °C for TGA analysis of HYNPs and CONPs. 5.76% percent weight loss in HYNPs was noted in the temperature range from room temperature to 50 °C. In the temperature range of room temperature to 70 °C, CONPs experience a 7% weight loss. That is brought on by absorbed moisture evaporating. Next, for both cases up to 320 °C, a loss of 3.8% and 6.8% for hydrothermal and co-precipitation NPs, respectively, is seen. This shows that the water molecules that the NPs had adsorbed have been removed. Finally, there is a weight loss of 2.6% for HYNPs and 1.4% for CONPs between 320 °C and 700 °C. This slight weight loss results from the burning of organic residues or the disintegration of agglomerated organic surface contaminants found in the NPs. Overall weight loss was detected for NPs created via the co-precipitation and hydrothermal methods to be 12.16% and 15.4%, respectively. Each sample has endothermic peaks according to the DSC thermograph. At 200 °C and 340 °C, respectively, two large endothermic peaks are seen for HYNPs. At 67 °C and 315 °C, respectively, two large endothermic peaks have been reported for CONPs [30, 32, 37].

The observed water evaporation and the dehydration of the dried organic matter are responsible for these endothermic peaks. The TGA and DSC curves of the related HYNPs and CONPs are shown in Figures 6(a) and (b), respectively. The thermal properties of NPs generated by hydrothermal and co-precipitation processes differ noticeably. In other words, HYNPs are more stable than CONPs up to 400 °C.

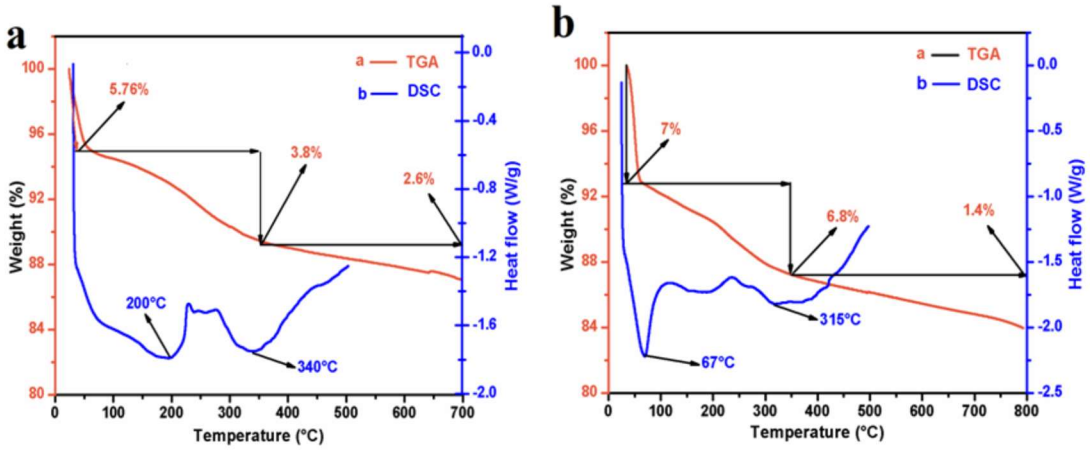

Figure-6

3.6 Biochemical processes

(3.6a). Antimicrobial evaluation

The generated CeO_2 NPs were tested for antimicrobial activity against the four harmful microorganisms. Gram negative Escherichia coli and Pseudomonas aeruginosa, as well as fungi Candida albicans, revealed Zones of Inhibition on the culture plates, demonstrating the NPs have high antibacterial strength. Gram positive bacteria Staphylococcus aureus and Bacillus subtilis also showed Zones of Inhibition. Cerium oxide nanoparticles' microbiological effectiveness often depends on factors like surface area, size, and shape. Reactive oxygen

SEYBOLD Report
ISSN: 1533 - 9211
DOI: 10.5281/zenodo.7236067

species (ROS) are produced as a result of the interaction between nanoparticles and microbes, which inhibits microbial growth and ultimately results in cell death.

Our data support the three types of interactions between bacteria and Ce NP proposed by Thill et al. [38]: adsorption, oxide diction, and toxicity. Here, we have demonstrated that HYNPs have stronger antibacterial properties than CONPs. The form of the nanoparticles is extremely important, as stated by Lian Wang et al. and Sang- Hoch et al. It has been claimed that the antibacterial effectiveness depends on more than just nanoparticles. Rather, it also depends on how the generated nanoparticles are shaped. There are morphological distinctions between HYNPs and CONPs, as we shown in Figures 5(a) and (c), which are TEM pictures of each kind of cell. The HYNPs have a cubic structure that resembles nanocubes and are uniformly distributed in nature. CONPs are aggregated, have a random orientation, and resemble nanoparticles or spheres.

We found that the hydrothermally created nanocubes had stronger bacterial activity than the co-precipitation technique created nanoparticles. The intermolecular interactions with bacteria change depending on the surface shape [39]. Therefore, based on shape, we may assume that HYNPs (nanocubes) will have more exposed stable reactive planes. According to reports, stable surface planes need extremely little energy to produce oxygen vacancies. As a result, HYNPs will interact well with bacteria, while CONPs (nanoparticles) have less exposed surface planes [40] and interact less with bacteria. This shows that, in comparison to CONPs, HYNPs have stronger antibacterial action to destroy microorganisms. Additionally, the compounds had significantly reduced antimicrobial action for yeast and significantly more antimicrobial activity for Gram-positive bacteria, indicating that these NPs are more potent antibacterial agents.

Additionally, we noticed concentration-dependent antibacterial activity. For the higher concentration, we saw a maximal zone of inhibition here, which is displayed in table 2. Figures 7(a), (b), (c), and (d) depict antimicrobial activities of CONPs for (C) B. subtilis and (D) C. albicans, respectively, as examples of antimicrobial activities (The highest zone of inhibition) of HYNPs for (A) B. subtilis and (B) C. albicans (d).

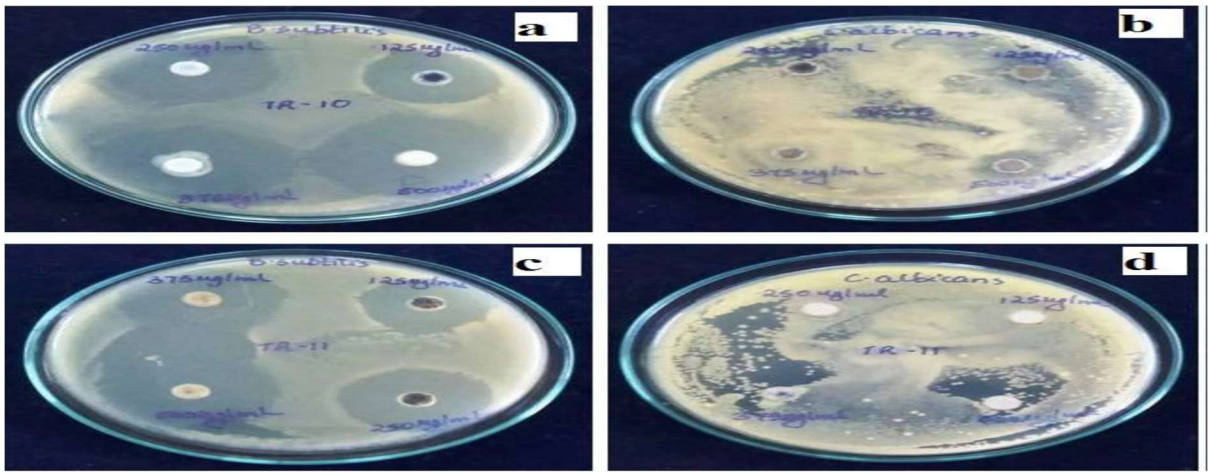

Figure – 7

(3.6b) Evaluation of antioxidants

SEYBOLD Report
ISSN: 1533 - 9211
DOI: 10.5281/zenodo.7236067

Ascorbic acid, HYNPs, and CONPs were evaluated for their ability to scavenge free radicals using the DPPH at five different concentrations (100, 200, 300, 400, and 500 g/ml). By comparing the absorbance at 517 nm to the blank, the residual DPPH could be measured, and the percent inhibition could be computed. Ascorbic acid, HYNPs, and CONPs' radical scavenging activity is assessed in figure 8 together with an error bar and a statistics bar that indicates the significance of the results. We discovered that there was a big disparity between the various materials. As concentration increased, the DPPH readings rose. The lowest concentration for HYNPs and CONPs was recorded at 100 g/ml, and their respective scavenging activities were 39.370.47 and 31.781.43, respectively. In contrast to CONPs, HYNPs had a higher level of scavenging activity. Due to its stronger antioxidant properties than CONPs, HYNPs may be effective in the treatment of a number of disorders.

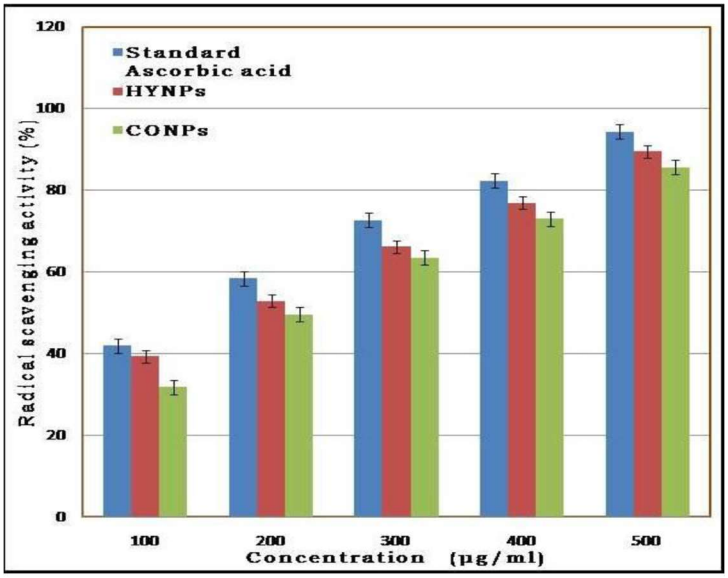

Figure – 8

4. Conclusion

The current analysis has found that the hydrothermal and coprecipitation methods were successful in producing CeO_2 NPs. The outcomes of the two approaches were examined and contrasted. Here, we recorded the results that follow; Initially, UV-Visible spectroscopy is used to validate the presence of CeO_2 NPs, and Tauc's plots show that HYNPs have a greater band gap energy than CONPs. FT-IR analysis showed that nitrates, Ce-O bands, O-H bands, and C-H bands were all present in the synthesised CeO_2 NPs made using the coprecipitation and hydrothermal methods.

The size of the produced CeO_2 NPs was established using XRD data; both have a face-centered cubic structure. Additionally, utilising XRD data, Scherrer's method, W-H method, and TEM analysis were used to calculate the crystallite size. Scherrer's, W-H, and TEM analyses of hydrothermally synthesised NPs show that they almost all have the same particle size, which strongly suggests that there is no particle aggregation and that the NPs are highly crystallized in nature. According to TGA/DSC experiments, HYNPs are significantly more stable than CONPs. For the four harmful bacteria, the HYNPs shown more effective antibacterial activity than the CONPs. Comparatively, HYNPs' antioxidant activities are

DOI: 10.5281/zenodo.7236067
stronger than CONPs'.

References

[1]. Auffan M, Rose J and Bottero J Y 2009 *Nat. Nanotechnol*4 634
[2]. Wu Z, Zhang J and Benfield R E 2002 *J Phys. Chem. B*106 4569
[3]. Trovarelli A, De Leitenburg C, Boaro M and Dolcetti G1999 *Catal.Today*50 353
[4]. Graziani M, Bekyarova E, Fornasiero P and Kas J 1998 *Catal .Today*45 179
[5]. Tsunekawa S, Sahara R, Kawazoe Y and atsuo kasuya2000 *Mater. Trans* 41 1104
[6]. Tsai M S 2004 *Mater .Sci. Eng B Solid-State Mater. Adv.Technol*110 132
[7]. Mori T, Wang Y and Drennan J 2004 *Solid State Ionics*175 641
[8. Li H, Wang G and Zhang F 2012 *RSC Adv 2* 12413
[9. Arul N S, Mangalaraj D and Han J I N 2015 *Bull MaterSci*38 1135
[10]. Tok A I Y, Boey F Y C, Dong Z and Sun X L 2007 *JMaterProcess Technol* 190 217
[11]. Pujar M S, Hunagund S M and Desai V R 2018 *62 ndAIP Conference Proceedings of DAE SSPS 2017* p 50026
[12]. Balavi H, Samadanian-isfahani S, Mehrabani-zeinabadMandEdrissi M 2013 *Powder Technol* 249 549
[13]. Masui T, Fujiwara K and Machida K I 1997 *Chem Mater*9 2197
[14]. Sharma V, Eberhardt K M and Sharma R 2010 *Chem PhysLett*495 280
[15]. Singh V, Karakoti A and Kumar A 2010 *J .Am. Ceram.Soc*93 3700
[16]. Nagy K and Dékány I 2009 *Colloids.Surfaces. APhysicochem .Eng .Asp* 345 31
[17]. Bumajdad A, Eastoe J and Mathew A 2009 *Adv. Colloid .Interface. Sci* 147 56
[18]. Qian L, Zhu J, Du W and Qian X 2009 *Mater. Chem. Phys*115 835
[19]. Gabal M A, Elroby S A K and Obaid A Y 2012 *PowderTechnol* 229 112
[20]. Njagi J, Ispas C and Andreescu S 2008 *Anal. Chem* 807266
[21]. Ispas C, Njagi J, Cates M and Andreescu S 2008 *J .Electrochem. Soc* 155 169[22]. Charbgoo F, Ramezani M and Darroudi M 2017 *Biosens. Bioelectron*96 33
[23]. Wang D, Kang Y and Doan-Nguyen V 2011 *AngewChemie - Int Ed* 50 4378
[24]. Deng W, Chen D, Hu J and Chen L 2015 *RSC. Adv* 5 80158
[25]. He L, Su Y, Lanhong J and Shi S 2015 *J Rare Earths* 33791
[26]. Walkey C, Das S and Seal S 2015 *Environ .Sci .Nano* 2 33
[27]. Caputo F, Mameli M and Sienkiewicz A 2017 *Sci .Rep*71
[28]. Hunagund S M, Desai V R and Barretto D A 2017 *J.Photochem .Photobiol. A Chem* 346 159
[29]. Sujana M G, Chattopadyay K K and Anand S 2008 *ApplSurf Sci* 254 7405
[30]. Babitha K K, Sreedevi A and Priyanka K P 2015 *Indian JPure Appl Phys* 53 596
[31]. John C 2000 IN r a Meyers (ed) Encyclopedia ofananlytical chemistry (John Wiley & Sons Ltd) p 10815

SEYBOLD Report
ISSN: 1533 - 9211
DOI: 10.5281/zenodo.7236067
[32]. JAYA K S K and N V 2013 *Asian J Chem* 25 6095
[33]. Kannan S K and Sundrarajan M 2014 *Int J Nanosci*131450018.
[34]. Khorsand Zak A, Abd. Majid W H, Abrishami M E andYousefi R 2011 *Solid State Sci* 13 251
[35]. Venkateswarlu K, Chandra Bose A and Rameshbabu N2010 *Phys .B .Condens. Matter* 405 4256
[36]. Hunagund S M, Desai V R and Barretto D A 2017 *Adv Sci Eng Med* 9 453
[37]. Chandradass J, Nam B and Kim K H 2009 *Colloids Surfaces APhysicochemEng Asp* 348 130
[38]. Antonie T, Ophelie Z, Olivier S, Franck C, Jernone R, Melaine A and Anne M F 2006 *Environ. Sci. Technol* 40 6151
[39]. Lian W, Hong H, Yunbo Y, Li S, Sijin L, Changbin Z and Lian H 2014 *J. of Inorg. Biochem 135 45*
[40] Sang-Ho C, Jin H, Matt M, Bongjun Y, J. Scott V and Nicholas A K 2015 *ACS, Nano 9 9097*